KnE Materials Science

ASRTU Conference Proceedings
IV Sino-Russian ASRTU Symposium on Advanced Materials and Processing Technology (2016), Volume 2016

Knowledge E
Engaging minds

Conference Paper

Controlling Surface Potential of Graphene Using dc Electric Field

R. Vidyasagar[1], B. Camargo[2], E. Pelegova[3], K. Romanyuk[1,3], and A.L. Kholkin[3]

[1]Physics Department & CICECO – Materials Institute of Aveiro, University of Aveiro, 3810-193 Aveiro, Portugal
[2]Physics Department, University of Leipzig, 04109 Leipzig, Germany
[3]Institute of Natural Sciences, Ural Federal University, 620000 Ekaterinburg, Russia

Abstract

In this work, we study surface potential of graphite deposited on SiO_2/Si substrate using Kelvin Probe Force Microscopy (KPFM) and Electric Force Microscopy (EFM). The amplitude modulated KPFM (AM-KPFM) shows that the graphene layer work function is 4.69±0.02 eV, whereas frequency modulated KPFM (FM-KPFM) revealed 4.50±0.02 eV. The work function indifference of 0.19±0.02 eV was attributed to the superior resolution of FM-KPFM and higher detection sensitivity of AM-KPFM. Subsequent EFM mapping suggests that the phase monotonically increases with increasing applied *dc* bias voltage in the range from -5 V to 5 V. This phase shift is ascribed to the induced charge polarization at tip-graphene surface due to interatomic interactions induced by *dc* field effects.

Keywords: Surface potential, graphene layers, *dc* field effects

Corresponding Author:
A.L. Kholkin; email:
kholkin@urfu.ru

Received: 9 September 2016
Accepted: 19 September 2016
Published: 12 October 2016

Publishing services provided by Knowledge E

Selection and Peer-review under the responsibility of the ASRTU Conference Committee.

OPEN ACCESS

1. Introduction

Carbon-based layered structures have been attractive to physicists in the last two decades as a testing ground for the manifestation of intriguing optical, electronic, and mechanical properties that would revolutionize the nano-electronic industry via development next-generation quantum transport in opto-electronic devices, nanoelectromechanical actuators, and biomedical sensors [1-5]. Contrastingly, low-dimension and linearly vanishing density of states at Dirac point of graphene suggests that each and every carbon atom is located at the surface, making graphene an attractive material for studying surface physics. Through the years, a variety of authors reported surface potential distribution between the single-layer graphene (1LG), double layer graphene (2LG), multi-layer graphene (MLG), and/or few layer graphene (FLG) transferred onto different substrates [6-9]. This contact potential difference between 1LG, 2LG, MLG, and FLG is controlled by ambient atmosphere, NO_2 environment, and substrate characteristics [10-11]. As a matter of fact, contact potential tuning is challenging in graphene, because electrostatic top-gate tends to degrade materials properties and the addition of chemical dopants or absorbents can cause unwanted disorder. To control these properties, electrostatic force microscopy (EFM) was used as a powerful tool to investigate graphene on different substrates, where accurate determination of flack height is less challenging, but the surface potential can be tuned

by the electric-field effects without fabricating top-gate electrodes [9, 12]. Although contact potential between 1LG and 2LG has been extensively studied, the knowledge of surface potential value of individual graphene layers has been very limited and unexplored [13].

In this article, by combining both Kelvin Probe Force Microscopy (KPFM) and EFM techniques, the surface potential distribution of graphene layers deposited on SiO_2 substrates has been demonstrated. AM-KPFM mapping showed the surface potential for the graphene as -0.33 V, whereas FM-KPFM imaging showed -0.54 V; the difference of 0.19 V could be attributed to the superior resolution of FM-KPFM and higher detection sensitivity of AM-KPFM. Significant monotonic increase of EFM phase is attributed to the contact potential of graphene caused by *dc* electric-field effect.

2. Methods

The used samples consist of mechanically exfoliated graphene/graphite transferred on to 300 nm thin SiO_2/Si substrates, where the back electrode Si is doped with N at the concentration of $10^{18}/cm^2$. A Solver Next commercial Atomic Force Microscope (AFM, NT-MDT, Russia) with cantilever having a conductive tip coated with Cr/Pt (resonant frequency 75 kHz and force constant 3 N/m) was used to characterize the graphene samples. In the first pass, the AFM tip traced the sample topography; subsequently, the surface potential mapping was performed in AM-KPFM mode (second pass mode). In FM-KPFM, the contact potential difference (CPD) was recorded along the same line scan in the second-pass mode while keeping the tip-surface distance of 10 nm. EFM is a two-pass mode, in which the electrostatic force between the charge on graphite and the tip is measured. The interatomic force is detected as a change in the resonant frequency with a corresponding phase shift as the cantilever experiences either attractive or repulsive force. In the present experiments, a lift height of h=50 nm is fixed above the surface to avoid topographic artifacts; the phase shift is imaged in the second-pass mode, while the *dc* bias applied to the probe. Schematic view of both KPFM and EFM is shown in Fig. 1.

3. Results

Figure 1a-f shows the topography and surface potential distribution features of a graphene layer obtained via both AM-KPFM and FM-KPFM mappings. The topography image of graphite/SiO_2 shows that the graphene layer is typically flat with small wrinkles and protrusions (Fig. 1a). The corresponding histogram profile indicates that the few layer graphene height is 10.19 nm, which is shown in Fig. 1b. Interestingly, both AM-KPFM and FM-KPFM images display slightly different contrast with much lower contact potential difference (ΔV_{CPD}) on the graphene layer in comparison with SiO_2 substrate (Fig. 1c,e), suggesting a smaller work function of graphene. To evaluate the ΔV_{CPD} of graphene, we plotted histogram profiles over the entire scanned area of Fig. 1d,f. The surface potential peak centered at 18 mV corresponds to the graphene layer, which is largely dark in contrast to the SiO_2 substrate of 344 mV. The evaluated

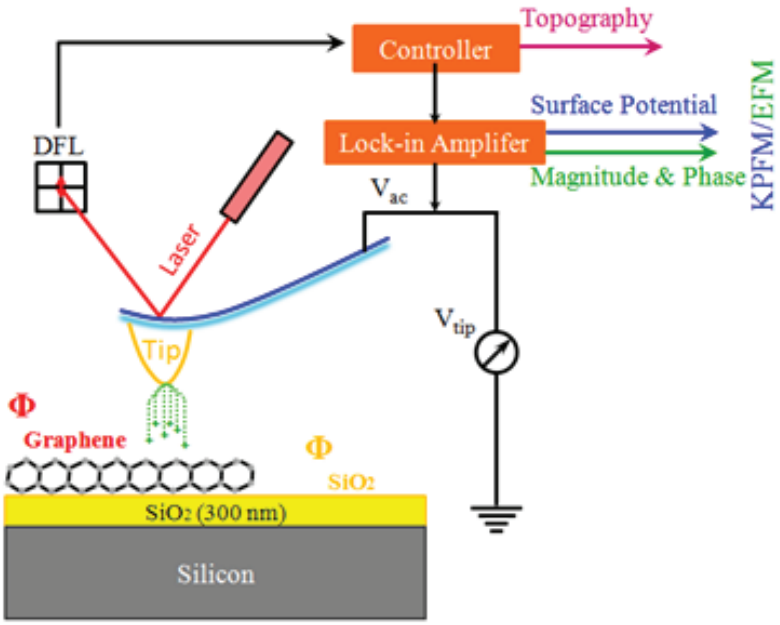

Figure 1: Schematic of the Kelvin Probe Force Microscopy and Electric Force Microscopy measurements in the structures graphene/SiO_2/Si.

ΔV_{CPD} between the SiO_2 and graphite is -0.33 V in AM-KPFM mode. Accordingly, the Gaussian distribution of peak position of graphene surface potential is 35 mV and the SiO_2 peak position is -570 mV, suggesting that the ΔV_{CPD} between the SiO_2 and FLG is about -0.54 V. The difference in the ΔV_{CPD} of graphene in AM-KPFM and FM-KPFM mode will be interpreted in the next section.

To evaluate the work function of graphene, initially we estimate the work function of the Cr/Pt coated tip by surface potential mapping on calibrated Highly Oriented Pyrolytic Graphite (HOPG) sample. The AM-KPFM and FM-KPFM mappings revealed that the work function of Cr/Pt tip is 5.02 eV and 5.04 eV respectively. The contact potential difference is defined as follows:

$$\Delta V_{CPD} = \frac{\psi_{tip} - \psi_{sample}}{-e} \quad (1)$$

where ψ_{tip} is the work function of the SPM tip, ψ_{sample} is the work function of the sample, e is the elementary charge, and ΔV_{CPD} is the measured contract potential difference.

Using this relation, we evaluated the graphene work function as 4.69±0.02 eV in AM-KPFM, whereas FM-KPFM revealed 4.50±0.02 eV. This work function value of 4.69 eV is in a good agreement with previously reported work function of 4.68 eV; hence, we suggest that this graphene is *p*-type band gap semiconductor [7, 11]. In addition, the work function value (4.50 ± 0.02 eV) of obtained in FM-SKPM is consistent with the value of 4.57±0.05 eV [10]. The difference of 0.19 eV in the work function is accounted by the fact that AM-KPFM has lower spatial resolution than FM-KPFM. In addition to that, slightly lower V_{CPD} value obtained from FM-KPFM is possibly due to a

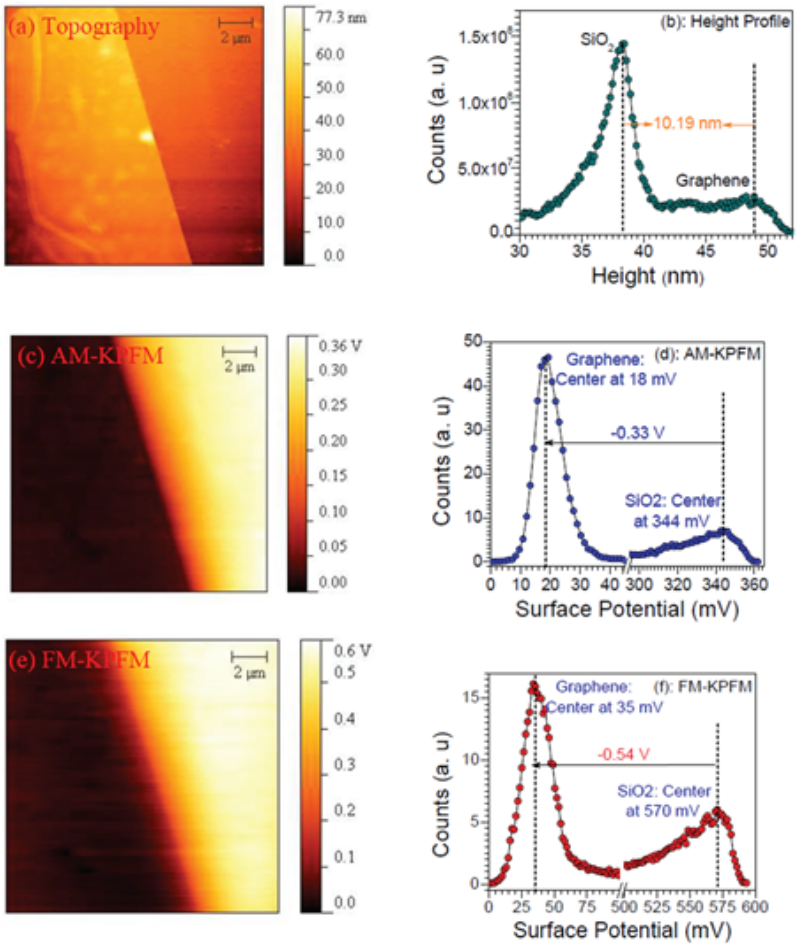

Figure 2: The topography (a, b) and surface potential characteristics of graphene layer transferred on SiO_2/Si using the AM-KPFM (c,d) and FM-KPFM (e,f). Left column represents corresponding maps and right column – histograms of topography and KPFM signal.

faintly larger tip-surface separation due to the additional *ac* bias and also of higher resolution capacity [13-14]. Higher sensitivity is important for the detection of the smallest changes in ΔV_{CPD} of very thin graphene layers; hence, AM-KPFM is better option to study work function of graphene.

Figure 3a,c shows the EFM phase images while applying the *dc* biases field of ± 4V to the probe; corresponding histogram profiles are shown in Fig. 3b,d. The phase contrast of graphene relative to SiO_2 substrate is always positive, indicating that our graphene is doped with holes in the ambient conditions. At V_{tip} = 4 V, the EFM phase for graphite is 5.48° and this phase is enhanced to 15.61°, while applying *dc* bias voltage of -4 V (Fig. 3b,d). We observed that the relative contrast between graphene is not reversed, even if the applied tip voltage has opposite polarity. But the relative phase contrast of graphene has improved much while applying negative *dc* bias fields, indicating that the EFM phase of graphene is more sensitive to negative *dc* field effects. Figure 3e shows the thickness dependence of EFM-phase of graphene layers, while the *dc* bias was applied to the tip (V_{tip}). Each EFM phase plot was obtained by performing 21 scans with different *dc* fields. Notably, the experimental plots of different thicknesses of graphite layers reveal a characteristic parabolic shape, which is in a good agreement with a

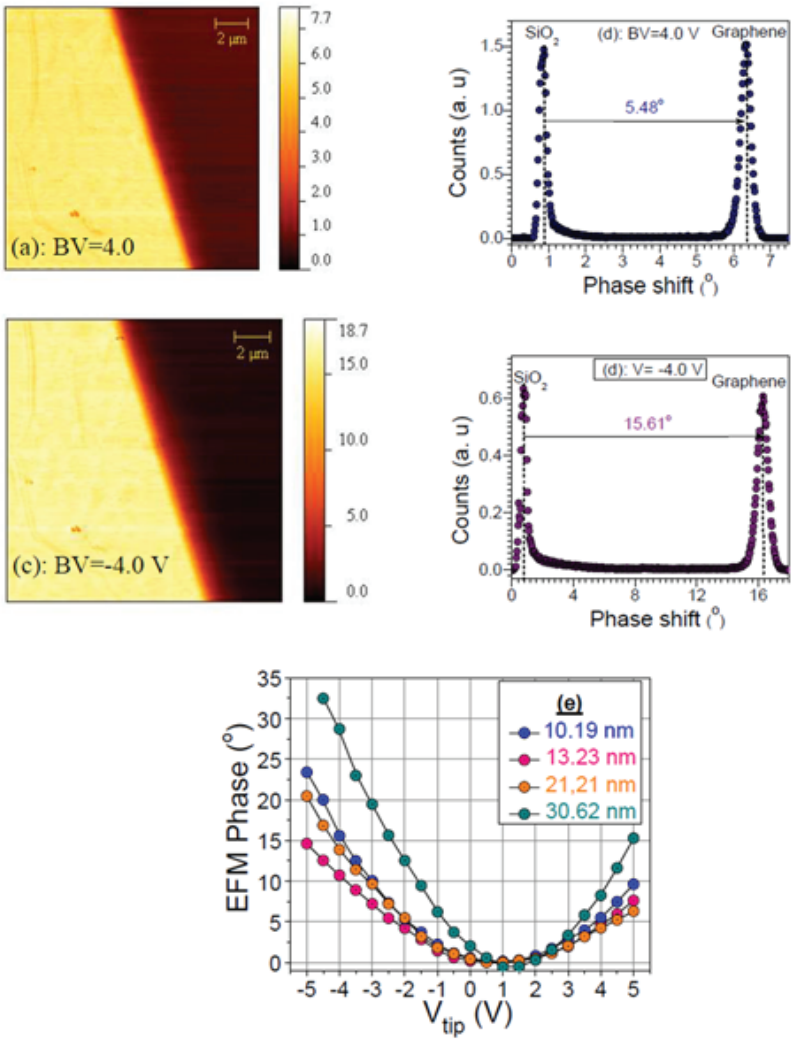

Figure 3: EFM phase of graphene layers on SiO_2/Si scanned, while *dc* voltage was applied to the probe: (a) EFM map, V = +4 V, (b) EFM histogram, V = +4 V, (c) EFM map, V = -4 V, (d) EFM histogram, V = -4 V, (e) voltage dependence of EFM phase for several thicknesses of graphene.

conventional model of capacitive coupling between the EFM probe and the sample is defined as:

$$\Delta\Phi(x,y) = -\frac{Q}{2k}C''(h)[V_{tip} - V_s(x,y)]^2 \quad (2)$$

where $\Delta\Phi(x,y)$ is the phase shift, Q and k are the quality factor and the spring constant of the cantilever, respectively, $C''(h)$ is the second derivative of the vertical distance between the tip-sample capacitance and the tip-bare substrate capacitance as a function of h, and $V_s(x,y)$ is the local electrostatic potential on the sample surface.

The phase shift in Eq. 2 is zero, when V_{tip} equals to the value of V_s. Generally, V_s is determined by the spatial distribution of charge carriers that are transferred to graphene from a thin buried layer of traps or defects in the SiO_2 substrate. From the relation, it is clear that the EFM phase shift corresponding to the surface potential distribution (V_s); hence, the monotonic increases of EFM phase ascribed to the increases of surface potential of graphite with the *dc* field effect up to ± 5 V. In contrast, external

contributions to the surface potential (e.g., such *p*-type adsorbates as water, oxygen, and hydrocarbons) lead to a uniform shift in the surface potential independent of the number of layers [12]. From our experimental data, the intrinsic modification of V_s corresponds to a steeper phase change originating from the shift of C 1*s* core level toward lower binding energies as the number of mono-atomic layers increases in graphene, assisted by the *dc* bias field effects applied to the probe [16].

4. Conclusion

In conclusion, we have demonstrated the local surface potential distribution of single-layer graphene deposited on SiO_2/Si substrate by employing Kelvin Probe Force Microscopy (KPFM), and Electric Force Microscopy (EFM). The AM-KPFM offers a straightforward identification of graphene layer work function of 4.74 eV whereas FM-KPFM revealed 4.59 eV, the difference of 0.19 eV in work function being attributed to the superior resolution of FM-KPFM and higher detection sensitivity of AM-KPFM. In contrast, we observed that the parabolic dependence of EFM phase with increase of *dc* electric field applied to the probe from 0 to $\pm$ 5 V. This phase shift of EFM phase is attributed to the variations of the surface electronic structure due to surface potential induced by the interatomic interaction between the electronic states of Cr/Pt tip and the graphene surface electrons.

Acknowledgements

R.V. thanks Foundation of Science and Technology of Portugal for the postdoctoral grant SFRH/BPD/104887/2014. E.P., K.R and A.L.K. are grateful to the Russian Foundation for Basic Research (grant No 16-29-14050-ofr-m) and Government of the Russian Federation (Act 211, Agreement 02.A03.21.0006) for the financial support. Part of this work was developed in the scope of Project CICECO-Aveiro Institute of Materials (ref. FCT UID/CTM/50011/2013), financed by national funds through the FCT/MEC and, when applicable, cofinanced by FEDER under the PT2020 Partnership Agreement.

References

[1] V. Meunier, AG. Souza Filho, and EB. Barros, Dresselhaus MS: Physical properties of low-dimensional sp2-based carbon nanostructures., Rev Mod Phys, *Rev Mod Phys*, **88**, Article ID 025005, (2016).

[2] A. H. Castro Neto, F. Guinea, N. M. R. Peres, K. S. Novoselov, and A. K. Geim, The electronic properties of graphene, *Reviews of Modern Physics*, **81**, no. 1, 109–162, (2009).

[3] N. M. Gabor, J. C. W. Song, Q. Ma, N. L. Nair, T. Taychatanapat, K. Watanabe, T. Taniguchi, L. S. Levitov, and P. Jarillo-Herrero, Hot carrier-assisted intrinsic photoresponse in graphene, *Science*, **334**, no. 6056, 648–652, (2011).

[4] G. Da Cunha Rodrigues, P. Zelenovskiy, K. Romanyuk, S. Luchkin, Y. Kopelevich, and A. Kholkin, Strong piezoelectricity in single-layer graphene deposited on SiO_2 grating substrates, *Nature Communications*, **6, article no. 7572**, (2015).

[5] Y. Liu, X. Dong, and P. Chen, Biological and chemical sensors based on graphene materials, *Chemical Society Reviews*, **41**, no. 6, 2283–2307, (2012).

[6] T. Yager, A. Lartsev, S. Mahashabde, S. Charpentier, D. Davidovikj, A. Danilov, R. Yakimova, V. Panchal, O. Kazakova, A. Tzalenchuk, S. Lara-Avila, and S. Kubatkin, Express optical analysis of epitaxial graphene on SiC: Impact of morphology on quantum transport, *Nano Letters*, **13**, no. 9, 4217–4223, (2013).

[7] R. Pearce, J. Eriksson, T. Iakimov, L. Hultman, A. Lloyd Spetz, and R. Yakimova, On the differing sensitivity to chemical gating of single and double layer epitaxial graphene explored using scanning kelvin probe microscopy, *ACS Nano*, **7**, no. 5, 4647–4656, (2013).

[8] T. Filleter, K. V. Emtsev, T. Seyller, and R. Bennewitz, Local work function measurements of epitaxial graphene, *Applied Physics Letters*, **93**, no. 13, Article ID 133117, (2008).

[9] Y.-J. Yu, Y. Zhao, S. Ryu, L. E. Brus, K. S. Kim, and P. Kim, Tuning the graphene work function by electric field effect, *Nano Letters*, **9**, no. 10, 3430–3434, (2009).

[10] D. Ziegler, P. Gava, J. Güttinger, F. Molitor, L. Wirtz, M. Lazzeri, A. M. Saitta, A. Stemmer, F. Mauri, and C. Stampfer, Variations in the work function of doped single- and few-layer graphene assessed by Kelvin probe force microscopy and density functional theory, *Physical Review B - Condensed Matter and Materials Physics*, **83**, no. 23, Article ID 235434, (2011).

[11] O. Kazakova, V. Panchal, and T. L. Burnett, Prevention of graphene restacking for performance boost of supercapacitors-a review, *Crystals*, **3**, no. 1, 191–233, (2013).

[12] T. Burnett, R. Yakimova, and O. Kazakova, Mapping of local electrical properties in epitaxial graphene using electrostatic force microscopy, *Nano Letters*, **11**, no. 6, 2324–2328, (2011).

[13] G. Cohen, E. Halpern, S. U. Nanayakkara, J. M. Luther, C. Held, R. Bennewitz, A. Boag, and Y. Rosenwaks, Reconstruction of surface potential from Kelvin probe force microscopy images, *Nanotechnology*, **24**, no. 29, Article ID 295702, (2013).

[14] P. Girard, Electrostatic force microscopy: Principles and some applications to semiconductors, *Nanotechnology*, **12**, no. 4, 485–490, (2001).

[15] F. Maeda, T. Takahashi, H. Ohsawa, S. Suzuki, and H. Suematsu, Unoccupied-electronic-band structure of graphite studied by angle-resolved secondary-electron emission and inverse photoemission, *Physical Review B*, **37**, no. 9, 4482–4488, (1988).

[16] H. Hibino, H. Kageshima, M. Kotsugi, F. Maeda, F.-Z. Guo, and Y. Watanabe, Dependence of electronic properties of epitaxial few-layer graphene on the number of layers investigated by photoelectron emission microscopy, *Physical Review B - Condensed Matter and Materials Physics*, **79**, no. 12, Article ID 125437, (2009).